Water Science & Technology

Water Science & Technology Vol 89 No 8, 2105 doi: 10.2166/wst.2024.104

Impact of PVC microplastics in photodynamic inactivation of *Staphylococcus aureus* and MRSA

Alessandra Ramos Lima [a,*], Kamila Jessie Sammarro Silva [a], Antônio Sérgio Nakao Aguiar [b,d], Mariana de Souza [a], Thalita Hellen Nunes Lima [a], Kate Cristina Blanco [a], Vanderlei Salvador Bagnato [a,c] and Lucas Danilo Dias [d]

[a] Laboratory of Environmental Biophotonics, São Carlos Institute of Physics, University of São Paulo, São Carlos, SP, Brazil
[b] Grupo de Química Teórica e Estrutural de Anápolis, Universidade Estadual de Goiás, Anápolis, GO, Brazil
[c] Department of Biomedical Engineering, Texas A&M University, College Station, TX, USA
[d] Laboratório de Novos Materiais, Universidade Evangélica de Goiás, Anápolis, GO, Brazil
*Corresponding author. E-mail: alessandra_lima@usp.br

ARL, 0000-0001-5810-5137; KJSS, 0000-0002-6881-4217; VSB, 0000-0003-4833-239X; LDD, 0000-0003-2858-7539

ABSTRACT

Photodynamic processes have found widespread application in therapies. These processes involve photosensitizers (PSs) that, when excited by specific light wavelengths and in the presence of molecular oxygen, generate reactive oxygen species (ROS), that target cells leading to inactivation. Photodynamic action has gained notable attention in environmental applications, particularly against pathogens and antibiotic-resistant bacteria (ARB) that pose a significant challenge to public health. However, environmental matrices frequently encompass additional contaminants and interferents, including microplastics (MPs), which are pollutants of current concern. Their presence in water and effluents has been extensively documented, highlighting their impact on conventional treatment methods, but this information remains scarce in the context of photodynamic inactivation (PDI) setups. Here, we described the effects of polyvinyl chloride (PVC) microparticles in PDI targeting *Staphylococcus aureus* and its methicillin-resistant strain (MRSA), using curcumin as a PS under blue light. The presence of PVC microparticles does not hinder ROS formation; however, depending on its concentration, it can impact bacterial inactivation. Our results underscore that PDI remains a potent method for reducing bacterial concentrations in water and wastewater containing ARB, even in highly contaminated scenarios with MPs.

Key words: methicillin-resistant *S. aureus*, antibiotic-resistant bacteria, curcumin, disinfection, polyvinyl chloride

HIGHLIGHTS

- Photodynamic inactivation is an effective tool against antibiotic resistance spread.
- The presence of microplastics hinders photodynamic inactivation up to a reversible point.
- A hypothesis on the photodynamic degradation of PVC is presented.

GRAPHICAL ABSTRACT

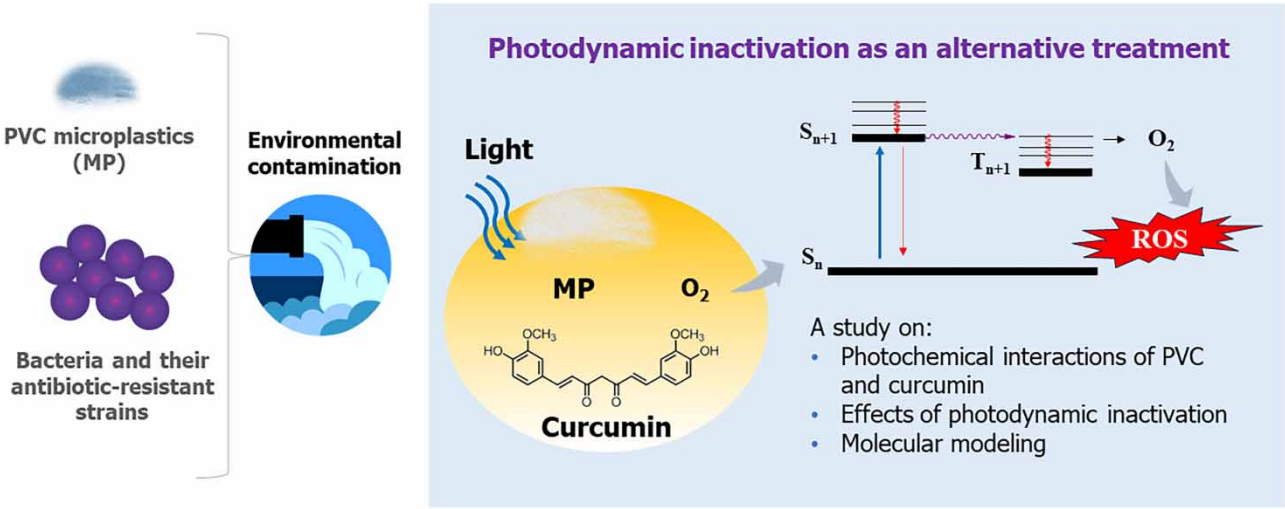

1. INTRODUCTION

The photodynamic process involves the use of a photosensitizer (PS) molecule, which, at the adequate wavelength of light and presence of oxygen, is able to produce reactive oxygen species (ROS), and singlet oxygen ($^1O_2$) by photophysical and photochemical mechanisms. The produced reactive species may react with biomolecules and induce to cell death (Robertson *et al.* 2009). This concept has been extended to various applications, including anticancer therapies (Dolmans *et al.* 2003) and antimicrobial treatments (Boltes Cecatto *et al.* 2020; Du *et al.* 2021), the degradation of chemical contaminants (Gmurek *et al.* 2017), and inactivation of public health significance, such as diseases vectors (Lima *et al.* 2022), pathogenic bacteria (Bartolomeu *et al.* 2017; Ugwuja *et al.* 2019), and antibiotic-resistant bacteria (ARB) (Sarker & Ahn 2022). In the context of ARB, photodynamic inactivation (PDI) assumes a pivotal role against its spread considering that it is a multitarget inactivation method that relies on oxidative stress (Almeida 2020).

In fact, existing literature presents evidence of the identification of ARB and their genetic components in water (Li *et al.* 2019), and wastewater treatment plants (Birošová *et al.* 2014; Rajabi *et al.* 2022). This underscores the potential significance of suggesting that PDI is a valuable tool for disinfection and tertiary treatment to counteract the prevalence of these microorganisms. Expanding on the environmental applications of PDI, it should be noted that it acts on complex matrices. These matrices often vary in physicochemical parameters, making their quality assessment an essential requirement for selecting the treatment technology (Silva *et al.* 2022). Different matrices may include specific pollutants that directly influence the mechanisms involved in the treatment train and operational units, presenting a challenge that extends to PDI as well (Almeida *et al.* 2014; Bartolomeu *et al.* 2023).

A topic that has been discussed in research on environmental pollution is the presence of microplastics (MPs) in different matrices. Upon disposal, plastic materials undergo various mechanisms leading to the formation of smaller particles measuring less than 5 mm (Zhang *et al.* 2021). MPs have been detected in various water sources such as seawater, freshwater, urban waterworks, treated tap water, and wastewater (Zhang *et al.* 2022; Wibuloutai *et al.* 2023; Yang *et al.* 2023). A recent study concluded that, along with feed water quality, the efficiency of the treatment plant is one of the major determinants of the vulnerability to contamination of treated water (Oladoja & Unuabonah 2021). The persistence of MPs after undertaking treatment has been demonstrated by numerous studies, which have consistently shown that MPs <0.3 mm often escape in primary and secondary treatment effluents (Blair *et al.* 2019; Pittura *et al.* 2021). Regarding tertiary treatment and disinfection, the presence of these contaminants has posed a notable challenge to the efficiency of membrane filtration, largely attributed to fouling mechanisms (Enfrin *et al.* 2020). Moreover, a recent paper elucidated that MPs caused a negative effect on UV inactivation of ARB (Manoli *et al.* 2022).

These reports raise questions on how MPs affect the efficiency of PDI against different microorganisms. This matter, to the authors' knowledge, has not been touched upon so far, particularly regarding curcumin as a PS, a natural-based compound

that has raised interest in PDI due to its high efficiency and low toxicity, which makes it friendly to environmental applications (Dias *et al.* 2020). Therefore, the aim of this study was to evaluate the effects of polyvinyl chloride (PVC) MPs on the performance of photodynamic water treatment against *Staphylococcus aureus* and methicillin-resistant *S. aureus*, using curcumin as a PS under blue light. Mechanisms were also investigated by photodegradation assays and theoretical molecular modeling.

2. METHODS

2.1. Chemicals and analytical methods

PVC MPs purchased from Sigma Aldrich MP suspensions were prepared in water, right before PDI assays.

Likewise, curcumin solutions were prepared immediately prior to antimicrobial assays. The powder was purchased from a commercial supplier (PDT Pharma, Brazil) and the master stock consisted of a dilution in ethanol 99.7% (Êxodo®, Brazil). Work solutions are further described. They were made out of dilutions of the master stock in autoclaved distilled water.

2.2. Scanning electronic microscopy

The morphological characteristics of MPs were analyzed by high-resolution scanning electron microscopy (FEG-SEM), with a field emission electron gun (FEG-SEM, Supra 35-VP, Carl Zeiss). The samples were fixed in the substrate on carbon tape, coated with gold/palladium and analyzed at 2.5 kV. Particle size measurement was performed using ImageJ software (version 1.50i). ImageJ software (National Institutes of Health, Bethesda, MD) was used to calculate the PVC MP average diameter.

2.3. Bacterial growth and quantification

PDI tests were carried out against two strains of bacteria: *S. aureus* (ATCC® 25923), and methicillin-resistant *S. aureus* (clinical isolate), given that previous research reported that they respond differently to PDI in terms of energy requirement (Sammarro Silva *et al.* 2023; Silva *et al.* 2023). Stocks were seeded onto Petri dishes containing brain-heart infusion (BHI) agar and incubated at 37 °C for 24 h. Grown colonies were resuspended in BHI broth, then incubated again at 37 °C for 24 h with no agitation. After this incubation period, aliquots were inoculated in BHI and grown to the mid-log phase. Growth was monitored by optical density (600 nm, Bel Photonics spectrophotometer) so that work suspensions of bacteria would be at ~10^7–10^8 colony forming units (CFUs) mL^{-1} for PDI experiments. Purification was done by centrifuging samples at 3,000 rpm for 15 min (Eppendorf 5,702 centrifuge) and the final pellets were suspended in 1× phosphate saline buffer (PBS, 7.4 pH). These suspensions undertook inactivation tests as detailed further.

After PDI assays, quantification was done by seeding aliquots of serial dilutions (in PBS) onto BHI agar plates, grown in the same conditions as previously stated, so that counts would be available in CFU mL^{-1}.

2.4. PDI experimental design and setup

Tests were performed *in vitro*, in sterile 24-well plates under fixed energy doses for each bacteria, i.e., 5 J cm^{-2} against *S. aureus* and 50 J cm^{-2} against MRSA, adapted from peer methodology and responding to the curcumin absorbance spectra (Almeida *et al.* 2017; Sammarro Silva *et al.* 2023; Silva *et al.* 2023). The PS sublethal concentrations were screened for both bacteria, considering: 3, 5, 7 and 10 μM of curcumin against *S. aureus* and against MRSA. These were repeated in the presence of PVC MPs. A simplified scheme of the experiments is shown in Figure 1.

In a typical experiment, each well was filled up with combinations of purified bacterial suspension (250 μL), MP suspension (250 μL) and PS solution (250 μL) in the desired concentrations. Prior to irradiation, the multi-well plates were incubated for 20 min at room temperature, under static conditions and protected from direct light. The selection concentrations of MP were based on extremely contaminated scenarios (0.25, 0.50, and 1.0 g L^{-1}), following similar research (Manoli *et al.* 2022) aimed at assessing the effects of the presence of such polymers in photonic disinfection methods.

Irradiation was performed using Biotable® device, which comprises 24 blue LEDs (emission peak at 450 nm, 41.05 mW cm^{-2} at the tested water level). Control experiments that did not contain any PVC (0.00 g L^{-1}) had their respective wells filled up to the same water head, by including the equivalent volume fraction of sterile deionized water. This is also applied for chemical toxicity and photochemical toxicity of MPs investigated in control experiments.

2.5. Photodegradation assays

A block of photodegradation assays targeted effects of irradiated PVC microparticles on the photobleaching of the PS molecule. In order to do so, suspensions of PVC in curcumin solution (10 μM; the highest PS concentration used) were irradiated

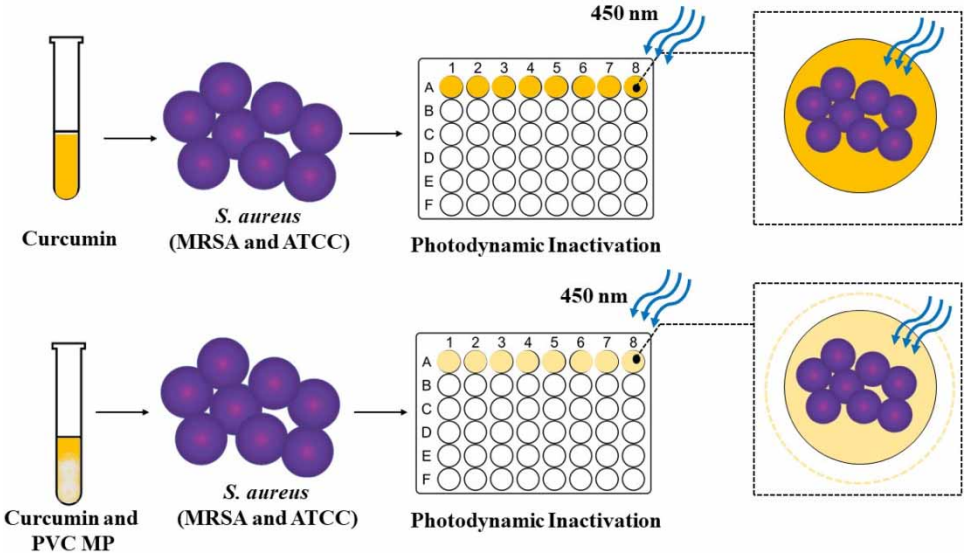

Figure 1 | Simplified diagram of photodynamic inactivation assays in the presence of PVC MPs.

under blue light (LED-based apparatus, emission peak at 450 nm, 21.6 mW cm^{-2}). Curcumin was quantified by UV-vis spectroscopy (Varian® Cary 50 UV-Vis spectrophotometer). The photodegradation percentage was calculated by a decrease in the maximum absorbance peak of the curcumin at 430 nm. Samples were collected under different light doses (0, 5, 10, 25, and 50 J cm^{-2}), aiming to provide a photodegradation kinetic profile.

Similarly, photodegradation assays targeting effects on the polymer were carried out. Curcumin (10 μM) and PVC (1.0 g L^{-1}; the highest tested concentration) were irradiated under blue LED light (450 nm, 41.05 mW cm^{-2}), at a specific light dose (50 J cm^{-2}), based on the UV-vis photodegradation assays. A control group with no irradiation was also considered. The aqueous solutions of the combinations of PVC and the PS were filtered through (7–12 μm) black band quantitative filter paper, aiming to concentrate the particles, and this material was left for drying at room temperature (28 °C, 24 h). The same procedure was performed for the PVC-curcumin suspension without irradiation. Analyses of curcumin powder, PVC, PVC-curcumin, PVC-light, and PVC-curcumin-light combinations were performed by Total Attenuated Fourier Transform Infrared Spectroscopy (ATR-FTIR), using a Cary 630 FTIR spectrophotometer (Agilent®, USA), spanning the scanning range of 650–4,000/cm with a resolution of 16 cm^{-1}.

2.6. Molecular modeling

To verify some chemical properties of PVC in the studied environment, theoretical calculations were simulated using density functional theory (DFT) (Hohenberg & Kohn 1964; Kohn & Sham 1965), implemented in the Gaussian 16 (Frisch *et al.* 2016) software package. The highly parameterized empirical exchange-correlation functional M06-2X (Zhao & Truhlar 2008) combined with the 6-311 + +G(d,p) polarized and diffuse basis set. For this, we built two linear PVC structures containing six monomers. The C atoms bonded to the Cl atom are chiral, and, therefore, in the first structure, these were arranged intercalated in the structure, while the second was constructed so that a sequence of three monomers contains C atoms with the same stereoisomerism (S–S–S). The f^0 Fukui function (Fukui 1982) calculations were used to verify possible sites of radical attacks in the PVC molecule, and through the Quantum Theory of Atoms in Molecules (QTAIM) (Bader 1985, 1994), possible interactions of the singlet oxygen molecule ($^1O_2$) present in the environment with PVC were verified. The topological parameters used were the electron density, $\rho(\mathbf{r})$, the Laplacian of the $\rho(\mathbf{r})$, $\nabla^2\rho(\mathbf{r})$, the kinetic, $G(\mathbf{r})$, and potential, $v(\mathbf{r})$, energies of the $\rho(\mathbf{r})$, and the total energy, $h(\mathbf{r})$. Finally, based on the analysis of the frontier molecular orbitals (Zhang & Musgrave 2007), the highest occupied molecular orbital (HOMO) and the lowest unoccupied molecular orbital (LUMO), it was possible to obtain chemical descriptors such as chemical potential (Pearson 1992):

$$\mu = \left(\frac{\partial E}{\partial N}\right)_v = -\frac{I + A}{2} = -\chi \tag{1}$$

a measure of charge transfer capacity, and chemical hardness (Pearson 2005):

$$\eta = \frac{1}{2}\left(\frac{\partial^2 E}{\partial N^2}\right)_v = \frac{I - A}{2} \tag{2}$$

a measure of resistance to deformation of the electron cloud during chemical processes. In Equations (1) and (2), E is the energy of the system, N is the number of particles, v is the external potential, χ is the electronegativity, $I \cong -E_{\mathrm{HOMO}}$ is the ionization potential, and $A \cong -E_{\mathrm{LUMO}}$ is the electron affinity.

2.7. Statistics

Inactivation data were checked for normal distribution using Shapiro–Wilk test (95% confidence interval). Normally distributed data were analyzed by Student's *t*-test for two samples so that toxicity and phototoxicity could be evaluated. Results on the effect of the presence of MPs in PDI were normalized by log-reduction and grouped into different blocks as per PS concentration and analyzed by one-way analysis of variance (ANOVA) ($\alpha = 0.05$).

3. RESULTS AND DISCUSSION

3.1. PVC MPs characterization

Figure 2(a) describes the overall morphology of PVC MPs used in this study, illustrating that they constitute spherical and semi-spherical particle shapes with large and irregular surfaces. The PVC particle diameter distribution is shown by the histogram in Figure 2(b), and it ranges from 40 to 200 μm, with an average value of 120 μm in particle size.

3.2. Effects of PVC MPs as a single factor

Table 1 provides the *p*-values resulting from the Student's *t*-tests of the toxicity and phototoxicity effects of MPs against both tested microorganisms. These are control groups for PVC standalone action. The statistical analyses were based on the residual CFUs corresponding to each specified illumination condition outlined in Table 1. The outcomes suggest no toxicity, except for the highest concentration of MPs against MRSA (contact time of 20 min 18 s). Notably, under light exposure, some degree of microorganism inactivation was detected, though never exceeding 1 log. This result could potentially be attributed to die-off or the photochemical effects to PVC that are further elucidated, given that blue light exposure to MRSA was not significantly toxic, though also led to 0.66 ± 0.08 log-reduction.

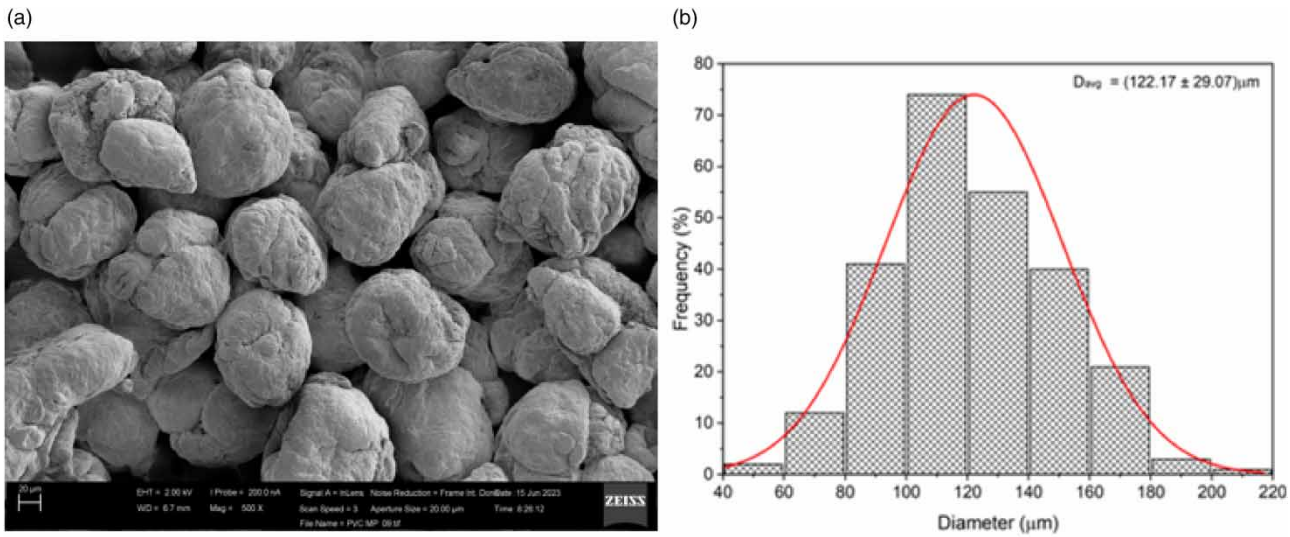

Figure 2 | (a) Scanning electron microscopy image of PVC MPs, scale bar refers to 200 μm, and (b) mean diameter distribution of PVC particles average value of 120 μm.

Table 1 | Student's *t* test *p*-values for toxicity and phototoxicity of PVC microplastics under different illumination setups

		Dark		Blue light	
Target	**MP (g L^{-1})**	**Log-inactivation ± SD**	***p*-value**	**Log-inactivation ± SD**	***p*-value**
S. aureus	0.00	0.00 ± 0.00	NA	0.00 ± 0.00	NA
	0.25	0.19 ± 0.17	0.1178	0.48 ± 0.09	**0.0018**
	0.50	0.15 ± 0.05	0.0718	0.60 ± 0.11	**< 0.001**
	1.00	0.17 ± 0.09	0.6456	0.34 ± 0.04	**0.0182**
MRSA	0.00	0.00 ± 0.00	NA	0.66 ± 0.08	0.0802
	0.25	0.09 ± 0.13	0.7468	0.23 ± 0.01	0.4060
	0.50	0.07 ± 0.12	0.5788	0.13 ± 0.12	0.7977
	1.00	0.69 ± 0.13	0.0313	0.70 ± 0.21	**0.0181**

Notes: SD refers to standard deviation. Results in bold refer to significant differences in means ($\alpha = 0.05$). Light dose against *S. aureus* and MRSA were 5 and 50 J cm^{-2}, respectively. NA = not applicable.

3.3. Influence of MPs in PDI

The overall effects of the presence of PVC MPs in antimicrobial photodynamic action are displayed in Figures 3 and 4, against *S. aureus* and MRSA, respectively. The efficiency of standalone PDI is shown by the dashed columns (absence of MP, i.e., PDI control groups). When comparing the effects of the sensitive strain to MRSA, the PDI treatment using curcumin was less effective than the latter. As the scope of the present study did not include mapping out operational conditions for optimal PDI, it should be noted that peer research has obtained improved log-reductions of MRSA in either planktonic or biofilm states, by adding higher concentrations or curcumin (and curcumin-based formulations) and/or increased light doses (Almeida *et al.* 2017; Araújo *et al.* 2018; Liu *et al.* 2018). Here, we worked with sublethal parameters so that we would be able to observe any changes caused by the presence of PVC as an interferent to the inactivation process.

For both targets, the presence of MPs in suspension hampered the PDI efficiency progressively. Nonetheless, at the highest concentration of MPs (1 g L^{-1}), results showed a recovery in photodynamic action, though not always reaching (and never surpassing) the full potential demonstrated by the absence of microparticles. The presence of suspended particles in photonic treatments is indeed expected to hinder inactivation efficiency. That is because they act on light scattering, attenuate energy delivery, and enable microorganisms to be shielded from irradiation (Emerick *et al.* 1999; Christensen & Linden 2003;

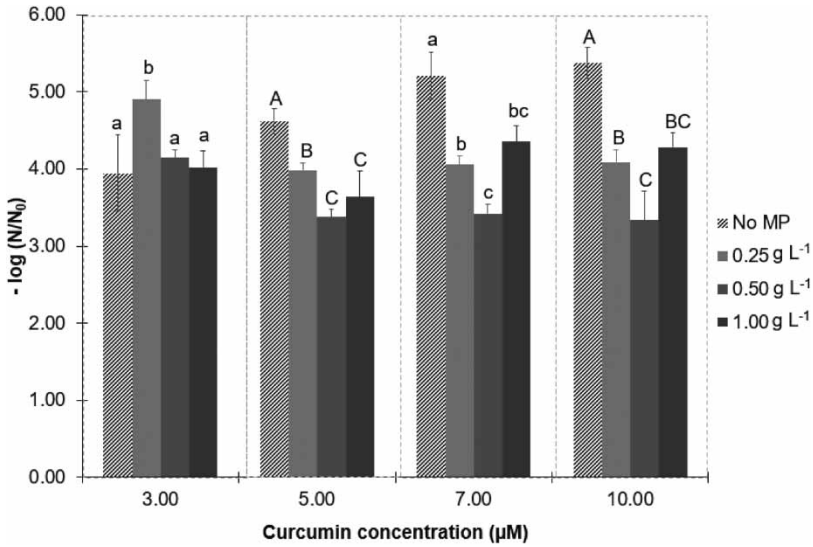

Figure 3 | Photodynamic inactivation of *S. aureus* using curcumin under blue light (5 J cm^{-2}) in the presence of PVC microplastics. *Notes*: relative log-reductions were first accounted for in CFU mL^{-1}. Statistical analyses were calculated by groups of curcumin concentration, identified by dashed blocks. The indication of the same character letters within a group refers to statistical similarity of means ($\alpha = 0.05$). Dark control groups for curcumin (10 μM) and its combination with PVC (1 g L^{-1}) led to log-removals of 0.08 ± 0.08, and 0.02 ± 0.13, respectively.

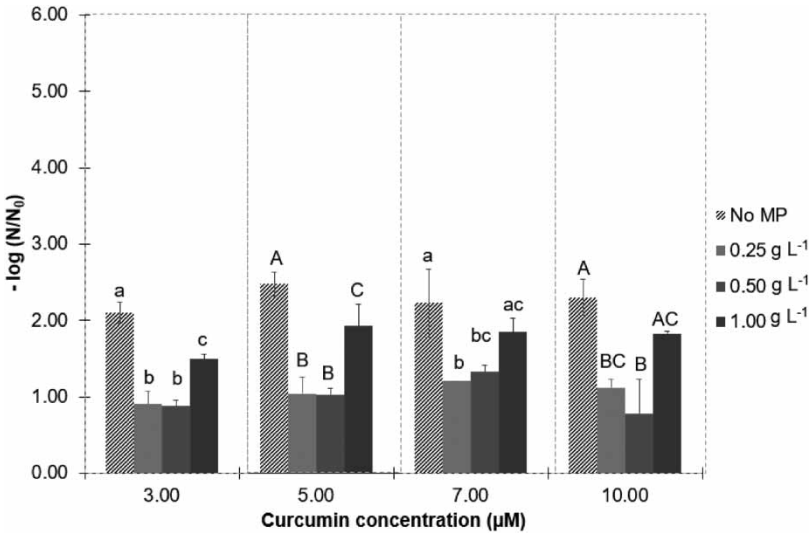

Figure 4 | Photodynamic inactivation of MRSA using curcumin under blue light (50 J cm^{-2}) in the presence of PVC microplastics. *Notes*: relative log-reductions were first accounted for in CFU mL^{-1}. Statistical analyses were calculated by groups of curcumin concentration, identified by dashed blocks. The indication of the same character letters within a group refers to statistical similarity of means ($\alpha = 0.05$). Dark control groups for curcumin (10 μM) and its combination with PVC (1 g L^{-1}) led to log-removals of 0.32 ± 0.05, and 0.29 ± 0.01, respectively.

Manoli *et al.* 2022). The efficiency of PDI using curcumin against both microorganisms, however, only dropped around 1 log-reduction, except for MRSA in the highest PS concentration. When adding 1 g L^{-1} PVC MPs to the system, though, we believe additional mechanisms took place to recover inactivation ability, as described in the following topics. This suggests that PDI using curcumin as an efficient approach against bacteria and ARB, even in MP-contaminated scenarios, but investigating details on the mechanisms involved is recommended for future research.

3.4. Photodegradation profiles

Figure 5 shows the photodegradation evaluation of curcumin in the presence of PVC (0, 0.25, 0.50, 1.0 g L^{-1}) using a set of light doses (0, 5, 10, 25, and 50 J cm^{-2}) at 450 nm. In all analyzed conditions, an increase in curcumin photodegradation was dependent on the light dose used (0–50 J cm^{-2}). Furthermore, in general, a proportional increase in the photodegradation of

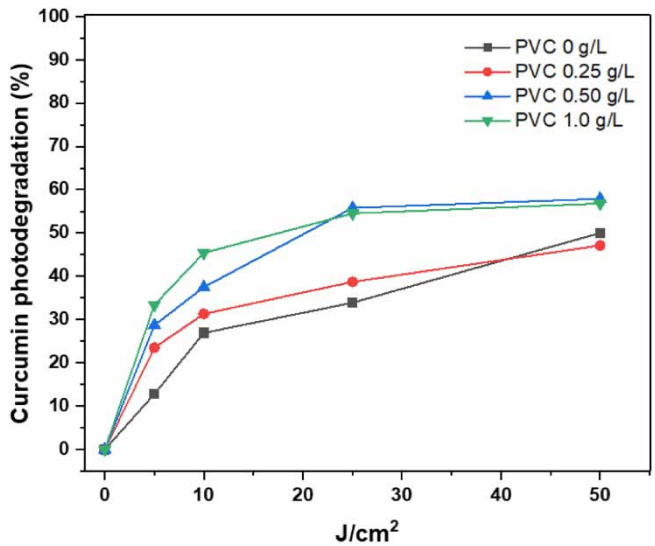

Figure 5 | Curcumin photodegradation profile in the presence of PVC under different light doses.

curcumin dependent on the PVC concentration in the medium was observed. The PVC concentration-dependent degradation of curcumin was mainly observed at light doses of 5, 10 and 25 J cm^{-2}. This higher curcumin photodegradation depending on PVC concentration may be explained by the formation of $Cl^{\cdot}$ and $H^{\cdot}$ reactive species *via* photoactivation of PVC surface by the light source and/or secondary reaction of ROS (such as $O_2^{-\cdot}$, $^{\cdot}OH$, H_2O_2, and $^1O_2$) with PVC (Castillo *et al.* 1990; Yang *et al.* 2011).

In summary, based on the photodegradation and photoinactivation data, we had expected a competitive process of the ROS produced, as previously reported (Dias *et al.* 2021). However, depending on PVC concentration, a recovery in PDI efficiency was found, considering results at lower levels of contamination with MPs. This observation may be explained by the formation of Cl. and H. species formed *via* hydrochlorination process at some specific settings (concentration of the contaminant vs. applied light dose). These reactive species present a high reactive property and may act as an antimicrobial tool in a cooperative way with the conventional ROS formed through a photodynamic process, depending on operational settings and contamination level. In certain conditions, however, they may also increase bleaching of the PS and hinder microbial inactivation, as shown by PDI assays against *S. aureus* and MRSA.

Figure 6 shows the photodegradation profiles of curcumin targeting effects on the polymer, under the highest energy dose (50 J cm^{-2}) at 450 nm. A comparison between FTIR spectra was performed accounting for (a) curcumin, (b) PVC, (c) irradiated PVC, (d) combined curcumin and PVC, and (e) combined curcumin and PVC after irradiation.

The (a) spectrum presents a band at 3,508 cm^{-1} attributed to the presence of the vibrational mode ν(O–H) of the phenolic group. At 1,625 cm^{-1}, the band attributed to ν(C = C) vibrations of the benzene ring bond. Another band at 1,598 cm^{-1} is attributed to the symmetric stretching vibrations of the benzene ring. At 1,506 cm^{-1} referring to the vibrational mode of the carbonyl ν(C = O). The band at 1,424 cm^{-1} olefinic bending vibrations ν(C-H). At 1,268 cm^{-1} vibrational stretching is attributed to aromaticity ν(C–O), while the band at 1,028 cm^{-1} refers to stretching vibrations ν(C–O–C). The bands at 954 and 715 cm^{-1} refer to the trans-CH vibrational modes of the benzoate and cis-CH of the aromatic ring, respectively (Mohan *et al.* 2012; Garbuio *et al.* 2022).

Spectrum (b) shows the FTIR for PVC with characteristic bands at 2,967–2,907 cm^{-1}, attributed to vibrational stretching ν(C–H) and at 1,423 cm^{-1} vibrational stretching of the $\nu(CH_3)$ group. The strain at 1,326 cm^{-1} refers to the vibrational

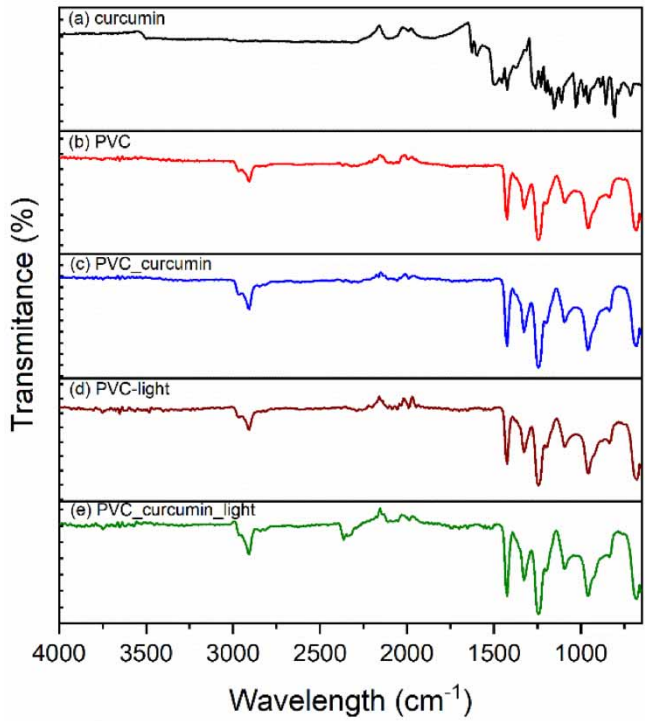

Figure 6 | FTIR spectra: (a) curcumin, (b) PVC, (c) PVC and curcumin, (d) blue light irradiated PVC, and (e) blue light irradiated PVC and curcumin combined (50 J cm^{-2} light dose).

mode $\nu(CH_2)$. The band at 1,252 cm^{-1} can be attributed to vibrational rocking $\nu(CH)$. At 961 cm^{-1}, the vibrational mode wagging trans-C–H and at 834 cm^{-1} vibrational stretching ν(C–Cl), while at 685 cm^{-1}, it is attributed to the vibrational mode cis-CH-wagging (Soman & Kelkar 2009; Kassem *et al.* 2023). There is no suggestion of curcumin adherence to the polymeric material, as spectrum (c), which refers to the combination PVC-curcumin that does not include the characteristic curcumin bands, though it includes the characteristic bands of the vibrational modes of the PVC polymer. PVC irradiated with a dose of 50 J cm^{-2} at 450 nm in the spectrum maintained its characteristic bands, as shown in Figure 6(d). Spectrum (e) showed the appearance of two bands in the regions of 2,366 and 2,340 cm^{-1}, without significant alteration in the other vibrations of PVC. This alteration may be associated with the photodegradation of the PVC polymer *via* singlet oxygen and free radical oxidation mechanisms (Lee & Li 2021), generated by the PS curcumin when irradiated by a light source at an appropriate wavelength (Dias *et al.* 2020). These are well-established mechanistic processes in the PDI of microorganisms, and our results suggest that an attack on PVC may also be taking place. At some operational conditions, the effects of this photodegradation may even be favorable for removing contaminants in general and maintaining the performance of PDI.

3.5. Interaction of ROS and PVC by molecular modeling

Calculations of the f^0 Fukui function showed that the chlorine atoms present in the PVC structure are favorable to attack by $^1O_2$ present in the environment. For the linear structure of PVC, where the stereochemistry is intercalated in R and S (PVC_1), it was observed that the f^0 values of the four central chlorine atoms are similar throughout the molecule. In the PVC_2 structure, whose C atoms have the same stereochemistry, it was observed that in the sequence S–S–S, the chlorine atom connected to the central carbon atom S (Figure 7), the f^0 function presented the highest value obtained, being the most likely location for these chemical attacks.

The formation of $^1O_2$ interactions with PVC stereoisomeric molecules was detected by the QTAIM formalism. The bond paths (BPs) showed the formation of interactions between O_2 and the Cl atoms bonded to the C_R atoms ($O\cdots Cl_R$) and to the H atom of the achiral C atom (O···H) for the PVC_1 stereoisomer, while in PVC2 observed the formation of an interaction with the Cl atom bonded to the C_S atom ($O\cdots Cl_S$) and with the H atoms of neighboring achiral C atoms (O···H). The topological parameters are presented in Table 2. Based on the results of Nakanishi *et al.* (2008, 2009), all observed interactions are van der Waals in nature, since $0.00 < \rho < 0.01$, $0.00 < \nabla^2\rho < 0.04$, and $0.000 < h < 0.002$. Furthermore, the ratio $|v|/G$ values are less than unity (Bader & Bader 1984; Cremer & Bock 1986), indicating that electrons are depleted in the region between two nuclear attractors, resulting in *closed-shell* interactions.

As shown in Table 3, compared to the results obtained for the PVC stereoisomers, $^1O_2$ has a very low LUMO energy (E_{LUMO}) and high electronic affinity (A), which may result in electron capture; moreover, $^1O_2$ has a low chemical hardness

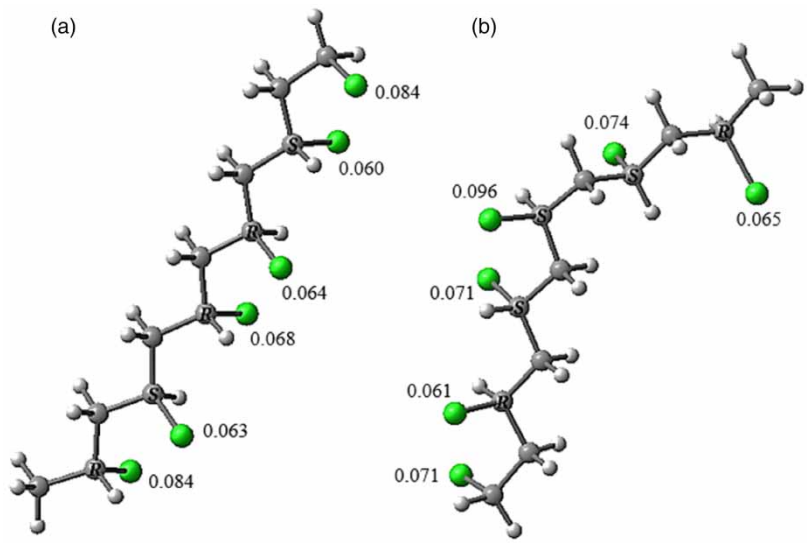

Figure 7 | Stereoisomeric linear forms of PVC, (a) PVC_1 and (b) PVC_2, with the values of the f^0 function of the Cl atoms.

Table 2 | QTAIM topological parameters for O_2···PVC interaction

BCP	Interaction	Distance (Å)	ρ (a.u.)	$\nabla^2\rho$ (a.u.)	$G(r)$ (a.u.)	$v(r)$ (a.u.)	$h(r)$ (a.u.)	$\frac{\lvert v\rvert}{G}$
				PVC_1				
			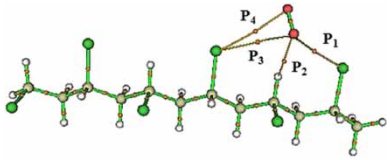					
P_1	O···Cl_R	3.469	0.0064	0.0225	0.0047	−0.0038	0.0009	0.8
P_2	O···H	2.457	0.0109	0.0357	0.0079	−0.0069	0.0010	0.9
P_3	O···Cl_R	3.474	0.0050	0.0192	0.0040	−0.0033	0.0008	0.8
P_4	O···Cl_R	3.429	0.0051	0.0197	0.0041	−0.0033	0.0008	0.8
				PVC_2				
			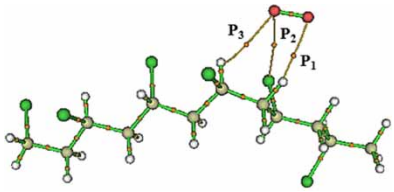					
P_1	O···H	2.516	0.0058	0.0205	0.0043	−0.0035	0.0008	0.8
P_2	O···Cl_S	3.391	0.0084	0.0301	0.0068	−0.0060	0.0008	0.9
P_3	O···H	2.604	0.0080	0.0274	0.0060	−0.0052	0.0008	0.9

BCP = bond critical point.

Table 3 | Reactivity indices for molecule $^1O_2$, and for enantiomeric forms of the PVC obtained at M06-2X/6-311 + +G(d,p) level of theory

Descriptor	O_2^1 (kcal mol^{-1})	PVC1 (kcal mol^{-1})	PVC2 (kcal mol^{-1})
E_{HOMO}	−209.630	−225.452	−224.430
E_{LUMO}	−68.441	−9.325	−7.613
$\Delta E^a_{H\text{-}L}$	141.190	216.127	216.817
Ionization energy (I)	209.630	225.452	224.430
Electronic affinity (A)	68.441	9.325	7.613
Electronegativity (χ)	139.035	117.388	116.021
Chemical potential (μ)	−139.035	−117.388	−116.021
Chemical hardness (η)	141.190	216.127	216.817

[a] $\Delta E_{H\text{-}L} = E_{LUMO} - E_{HOMO}$.

and can become polarized (this justifies the weak interaction with PVC). On the other hand, the polymer has high chemical potential, being able to transfer charge to $^1O_2$.

4. CONCLUSIONS

The primary aim of this study was to evaluate the impact of PVC MPs on PDI targeting *S. aureus* and its methicillin-resistant strain (MRSA) in water matrices. Conducted in a controlled *in vitro* environment, the investigation employed curcumin as the PS and blue light for operation conditions, and high concentrations of MPs to replicate highly contaminated scenarios.

Our findings showed a concentration-dependent hindrance effect exerted by MPs on the efficacy of microorganism inactivation for both *S. aureus* and its MRSA. This trend was corroborated by photodegradation assays of the PS and was further

influenced by the dependence on light energy dosage. Notably, at the highest contamination level, a reversal in photodynamic action was noted, manifesting as an enhancement in inactivation compared to instances with lower PVC concentrations. This recovery was attributed to the formation of supplementary reactive species, a notion validated by the profiles obtained through PS photodegradation assays and supported by theoretical molecular modeling.

Our outcomes highlight PDI as a potential tool for microorganism and ARB control in the contexts of water disinfection and wastewater tertiary treatment, even when confronted with PVC microplastic contamination. Notably, while the presence of MPs does impede efficiency up to a reversible threshold, the processes underpinning photodynamic action extend beyond microorganism inactivation, also applying to the degradation of polymeric contaminants. However, methodological limitations apply to the present paper, inviting future research aimed at elucidating the mechanisms involved in this change from competition to a suggested improvement in PDI efficiency in the presence of PVC as a contaminant. Tests on real environmental matrices and other PS molecules are also encouraged.

ACKNOWLEDGEMENTS

The authors are grateful to the Fundação de Amparo à Pesquisa do Estado de Goiás (FAPEG) (201810267001556 and Inovação, Desenvolvimento e Sustentabilidade: Estreitamento entre Universidade e Setor Produtivo no Estado de Goiás Convênio para pesquisa, desenvolvimento e inovação – PD&I 07/2020), Coordenação de Aperfeiçoamento de Pessoal de Nível Superior (CAPES) (88887.710665/2022-00, 8887.820460/2023-00). The authors also thank Fundação de Amparo à Pesquisa do Estado de São Paulo (FAPESP) (CEPOF 2013/07276-1, 2023/11853–6) and INCT 'Basic Optics and Applied to Life Sciences' (FAPESP 2014/50857-8, Conselho Nacional de Desenvolvimento e Pesquisa – CNPq 465360/2014-9). USA agencies also supported this work: GURI -M2303930, CPRIT-RR220054 and CRI-29034.

DATA AVAILABILITY STATEMENT

All relevant data are included in the paper or its Supplementary Information.

CONFLICT OF INTEREST

The authors declare there is no conflict.

REFERENCES

Almeida, A. 2020 Photodynamic therapy in the inactivation of microorganisms. *Antibiotics* **9**, 138. doi:10.3390/antibiotics9040138.

Almeida, J., Tomé, J. P. C., Neves, M. G. P. M. S., Tomé, A. C., Cavaleiro, J. A. S., Cunha, Â., Costa, L., Faustino, M. A. F. & Almeida, A. 2014 Photodynamic inactivation of multidrug-resistant bacteria in hospital wastewaters: Influence of residual antibiotics. *Photochemical and Photobiological Sciences* **13**, 626–633. doi:10.1039/C3PP50195G.

Almeida, P. P., Pereira, Í. S., Rodrigues, K. B., Leal, L. S., Marques, A. S., Rosa, L. P., da Silva, F. C. & da Silva, R. A. A. 2017 Photodynamic therapy controls of *Staphylococcus aureus* intradermal infection in mice. *Lasers in Medical Science* **32**, 1337–1342. doi:10.1007/s10103-017-2247-1.

Araújo, T. S. D., Rodrigues, P. L. F., Santos, M. S., De Oliveira, J. M., Rosa, L. P., Bagnato, V. S., Blanco, K. C. & Da Silva, F. C. 2018 Reduced methicillin-resistant *Staphylococcus aureus* biofilm formation in bone cavities by photodynamic therapy. *Photodiagnosis and Photodynamic Therapy* **21**, 219–223. doi:10.1016/j.pdpdt.2017.12.011.

Bader, R. F. W. 1985 Atoms in molecules. *Accounts of Chemical Research* **18**, 9–15. doi:10.1021/ar00109a003.

Bader, R. F. W. 1994 *Atoms in Molecules: A Quantum Theory*. International Ser. of Monogr. on Chem. Clarendon Press, Oxford. ISBN 978-0-19-855865-1.

Bader, R. F. W. & Bader, R. F. W. 1984 The characterization of atomic interaction. *The Journal of Physical Chemistry* **80**, 1943–1960. doi:10.1063/1.446956.

Bartolomeu, M., Reis, S., Fontes, M., Neves, M. G. P. M. S., Faustino, M. A. F. & Almeida, A. 2017 Photodynamic action against wastewater microorganisms and chemical pollutants: An effective approach with low environmental impact. *Water* **9**, 630. doi:10.3390/w9090630.

Bartolomeu, M., Monteiro, C. J. P., Fontes, M., Neves, M. G. P. M. S., Faustino, M. A. F. & Almeida, A. 2023 Photodynamic inactivation of microorganisms in different water matrices: The effect of physicochemical parameters on the treatment outcome. *Science of the Total Environment* **860**, 160427. doi:10.1016/j.scitotenv.2022.160427.

Birošová, L., Mackuľak, T., Bodík, I., Ryba, J., Škubák, J. & Grabic, R. 2014 Pilot study of seasonal occurrence and distribution of antibiotics and drug resistant bacteria in wastewater treatment plants in Slovakia. *Science of the Total Environment* **490**, 440–444. doi:10.1016/j.scitotenv.2014.05.030.

Blair, R. M., Waldron, S. & Gauchotte-Lindsay, C. 2019 Average daily flow of microplastics through a tertiary wastewater treatment plant over a ten-month period. *Water Research* **163**, 114909. doi:10.1016/j.watres.2019.114909.

Boltes Cecatto, R., Siqueira de Magalhães, L., Fernanda Setúbal Destro Rodrigues, M., Pavani, C., Lino-dos-Santos-Franco, A., Teixeira Gomes, M. & Fátima Teixeira Silva, D. 2020 Methylene blue mediated antimicrobial photodynamic therapy in clinical human studies: The state of the art. *Photodiagnosis and Photodynamic Therapy* **31**, 101828. doi:10.1016/j.pdpdt.2020.101828.

Castillo, F., Martínez, G., Sastre, R., Millán, J., Bellenger, V., Gupta, B. D. & Verdu, J. 1990 Influence of structure on the photo-degradation of PVC. Part IV – a conclusive approach to the mechanism of photo-oxidation and photo-dehydrochlorination. *Polymer Degradation and Stability* **27**, 1–11. doi:10.1016/0141-3910(90)90092-L.

Christensen, J. & Linden, K. G. 2003 How particles affect UV light in the UV disinfection of unfiltered drinking water. *Journal AWWA* **95**, 179–189. doi:10.1002/j.1551-8833.2003.tb10344.x.

Cremer, D. & Bock, C. W. 1986 Theoretical determination of molecular structure and conformation. 18. The formation of epoxides during the ozonolysis of alkenes. *Journal of the American Chemical Society* **108**, 3375–3379. doi:10.1021/ja00272a036.

Dias, L. D., Blanco, K. C., Mfouo-Tynga, I. S., Inada, N. M. & Bagnato, V. S. 2020 Curcumin as a photosensitizer: From molecular structure to recent advances in antimicrobial photodynamic therapy. *Journal of Photochemistry and Photobiology C: Photochemistry Reviews* **45**, 100384. doi:10.1016/j.jphotochemrev.2020.100384.

Dias, L. D., Corrêa, T. Q. & Bagnato, V. S. 2021 Cooperative and competitive antimicrobial photodynamic effects induced by a combination of methylene blue and curcumin. *Laser Physics Letters* **18**, 075601. doi:10.1088/1612-202X/ac0981.

Dolmans, D., Fukumura, D. & Jain, R. K. 2003 Photodynamic therapy for cancer. *Nature Reviews Cancer* 380–387. doi:10.1038/nrc1071.

Du, M., Xuan, W., Zhen, X., He, L., Lan, L., Yang, S., Wu, N., Qin, J., Zhao, R., Qin, J., Lan, J., Lu, H., Liang, C., Li, Y., Hamblin, M. & Huang, L. 2021 Antimicrobial photodynamic therapy for oral candida infection in adult AIDS patients: A pilot clinical trial. *Photodiagnosis and Photodynamic Therapy* **34**, 102310. doi:10.1016/j.pdpdt.2021.102310.

Emerick, R. W., Loge, F. J., Thompson, D. & Darby, J. L. 1999 Factors influencing ultraviolet disinfection performance part II: Association of coliform bacteria with wastewater particles. *Water Environment Research* **71**, 1178–1187. doi:10.2175/106143097X122004.

Enfrin, M., Lee, J., Le-Clech, P. & Dumée, L. F. 2020 Kinetic and mechanistic aspects of ultrafiltration membrane fouling by nano- and microplastics. *Journal of Membrane Science* **601**, 117890. doi:10.1016/j.memsci.2020.117890.

Frisch, M. J., Trucks, G. W., Schlegel, H. B., Scuseria, G. E., Robb, M. A., Cheeseman, J. R., Scalmani, G., Barão, V., Petersson, G. A., Nakatsuji, H., Li, X., Caricato, M., Marenich, A. V., Bloino, J., Janesko, B. G., Gomperts, R., Mennucci, B., Hratchian, H. P., Ortiz, J. V., Izmaylov, A. F., Sonnenberg, J. L., Williams-Young, D., Ding, F., Lipparini, F., Egidi, F., Goings, J., Peng, B., Petrone, A., Henderson, T., Ranasinghe, D., Zakrzewski, V. G., Gao, J., Rega, N., Zheng, G., Liang, W., Hada, M., Ehara, M., Toyota, K., Fukuda, R., Hasegawa, J., Ishida, M., Nakajima, T., Honda, Y., Kitao, O., Nakai, H., Vreven, T., Throssell, K., Montgomery Jr., J. A., Peralta, J. E., Ogliaro, F., Bearpark, M. J., Heyd, J. J., Brothers, E. N., Kudin, K. N., Staroverov, V. N., Keith, T. A., Kobayashi, R., Normand, J., Raghavachari, K., Rendell, A. P., Burant, J. C., Iyengar, S. S., Tomasi, J., Cossi, M., Millam, J. M., Klene, M. , Adamo, C., Cammi, R., Ochterski, J. W., Martin, R. L., Morokuma, K., Farkas, O., Foresman, J. B., Fox, D. J. & Gaussian, Inc., Wallingford CT 2016 *GaussView 5.0.* EUA, Wallingford.

Fukui, K. 1982 Role of frontier orbitals in chemical reactions. *Science* **218**, 747–754. doi:10.1126/science.218.4574.

Garbuio, M., Dias, L. D., de Souza, L. M., Corrêa, T. Q., Mezzacappo, N. F., Blanco, K. C., de Oliveira, K. T., Inada, N. M. & Bagnato, V. S. 2022 Formulations of curcumin and D-Mannitol as a photolarvicide against *Aedes aegypti* larvae: Sublethal photolarvicidal action, toxicity, residual evaluation, and small-scale field trial. *Photodiagnosis and Photodynamic Therapy* **38**, 102740. doi:10.1016/j.pdpdt.2022.102740.

Gmurek, M., Foszpańczyk, M., Olak-Kucharczyk, M., Gryglik, D. & Ledakowicz, S. 2017 Photosensitive chitosan for visible-light water pollutant degradation. *Chemical Engineering Journal* **318**, 240–246. doi:10.1016/j.cej.2016.06.125.

Hohenberg, P. & Kohn, W. 1964 Inhomogeneous electron gas. *Physical Review* **136**, B864–B871. doi:10.1103/PhysRev.136.B864.

Kassem, S. M., Abdel Maksoud, M. I. A., El Sayed, A. M., Ebraheem, S., Helal, A. I. & Ebaid, Y. Y. 2023 Optical and radiation shielding properties of PVC/$BiVO_4$ nanocomposite. *Scientific Reports* **13**, 10964. doi:10.1038/s41598-023-37692-y.

Kohn, W. & Sham, L. J. 1965 Self-consistent equations including exchange and correlation effects. *Physical Review* **140**, A1133–A1138. doi:10.1103/PhysRev.140.A1133.

Lee, Q. Y. & Li, H. 2021 Photocatalytic degradation of plastic waste: A mini review. *Micromachines* **12**, 907. doi:10.3390/mi12080907.

Li, R., Jay, J. A. & Stenstrom, M. K. 2019 Fate of antibiotic resistance genes and antibiotic-resistant bacteria in water resource recovery facilities. *Water Environment Research* **91**, 5–20. doi:10.1002/wer.1008.

Lima, A. R., Dias, L. D., Garbuio, M., Inada, N. M. & Bagnato, V. S. 2022 A look at photodynamic inactivation as a tool for pests and vector-borne diseases control. *Laser Physics Letters* **19**, 025601. doi:10.1088/1612-202X/ac4591.

Liu, J., Yu, M., Zeng, G., Cao, J., Wang, Y., Ding, T., Yang, X., Sun, K., Parvizi, J. & Tian, S. 2018 Dual antibacterial behavior of a curcumin–upconversion photodynamic nanosystem for efficient eradication of drug-resistant bacteria in a deep joint infection. *Journal of Materials Chemistry B* **6**, 7854–7861. doi:10.1039/C8TB02493F.

Manoli, K., Naziri, A., Ttofi, I., Michael, C., Allan, I. J. & Fatta-Kassinos, D. 2022 Investigation of the effect of microplastics on the UV inactivation of antibiotic-resistant bacteria in water. *Water Research* **222**, 118906. doi:10.1016/j.watres.2022.118906.

Mohan, P. R. K., Sreelakshmi, G., Muraleedharan, C. V. & Joseph, R. 2012 Water soluble complexes of curcumin with cyclodextrins: Characterization by FT-Raman spectroscopy. *Vibrational Spectroscopy* **62**, 77–84. doi:10.1016/j.vibspec.2012.05.002.

Nakanishi, W., Hayashi, S. & Narahara, K. 2008 Atoms-in-molecules dual parameter analysis of weak to strong interactions: Behaviors of electronic energy densities versus Laplacian of electron densities at bond critical points. *The Journal of Physical Chemistry A* **112**, 13593–13599. doi:10.1021/jp8054763.

Nakanishi, W., Hayashi, S. & Narahara, K. 2009 Polar coordinate representation of Hb(Rc) versus ($\hbar$2/8 m)$\bigtriangledown$2ρb(Rc) at BCP in AIM analysis: Classification and evaluation of weak to strong interactions. *The Journal of Physical Chemistry A* **113**. doi:10.1021/jp903622a.

Oladoja, N. A. & Unuabonah, I. E. 2021 The pathways of microplastics contamination in raw and drinking water. *Journal of Water Process Engineering* **41**, 102073. doi:10.1016/j.jwpe.2021.102073.

Pearson, R. G. 1992 The electronic chemical potential and chemical hardness. *Journal of Molecular Structure: THEOCHEM* **255**, 261–270. doi:10.1016/0166-1280(92)85014-C.

Pearson, R. G. 2005 Chemical hardness and density functional theory. *Journal of Chemical Sciences* **117**, 369–377. doi:10.1007/BF02708340.

Pittura, L., Foglia, A., Akyol, Ç., Cipolletta, G., Benedetti, M., Regoli, F., Eusebi, A. L., Sabbatini, S., Tseng, L. Y. Katsou, E., Gorbi, S. & Fatone, F. 2021 Microplastics in real wastewater treatment schemes: Comparative assessment and relevant inhibition effects on anaerobic processes. *Chemosphere* **262**, 128415. doi:10.1016/j.chemosphere.2020.128415.

Rajabi, A., Farajzadeh, D., Dehghanzadeh, R., Aslani, H., Mousavi, S., Mosaferi, M., Dehghani, M. H. & Asghari, F. B. 2022 Characterization of antibiotic resistance genes and bacteria in a municipal water resource recovery facility. *Water Environment Research* **94**, e10750. Wiley Online Library Available from: https://onlinelibrary.wiley.com/doi/full/10.1002/wer.10750 (accessed on 27 June 2023).

Robertson, C. A., Evans, D. H. & Abrahamse, H. 2009 Photodynamic therapy (PDT): A short review on cellular mechanisms and cancer research applications for PDT. *Journal of Photochemistry and Photobiology B: Biology* **96**, 1–8. doi:10.1016/j.jphotobiol.2009.04.001.

Sammarro Silva, K. J., Lima, A. R., Dias, L. D., De Souza, M., Nunes Lima, T. H. & Bagnato, V. S. 2023 Hydrogen peroxide preoxidation as a strategy for enhanced antimicrobial photodynamic action against methicillin-resistant *Staphylococcus aureus*. *Journal of Water and Health* **21**, 1922–1932. doi:10.2166/wh.2023.245.

Sarker, M. A. R. & Ahn, Y.-H. 2022 Photodynamic inactivation of multidrug-resistant bacteria in wastewater effluent using green phytochemicals as a natural photosensitizer. *Environmental Pollution* **311**, 120015. doi:10.1016/j.envpol.2022.120015.

Silva, K. J. S., Leite, L. d. S., Fava, N. d. M. N., Daniel, L. A. & Sabogal-Paz, L. P. 2022 Effects of hydrogen peroxide preoxidation on clarification and reduction of the microbial load of groundwater and surface water sources for household treatment. *Water Supply* **22**, 2977–2987. doi:10.2166/ws.2021.421.

Silva, K. J. S., Lima, A. R., Corrêa, T. Q., Dias, L. D. & Bagnato, V. S. 2023 Hydrogen peroxide as an additive to curcumin on the photodynamic inactivation of bacteria: A preliminary study. *Laser Physics* **33**, 085601. doi:10.1088/1555-6611/acde71.

Soman, V. V. & Kelkar, D. S. 2009 FTIR studies of doped PMMA – PVC blend system. *Macromolecular Symposia* **277**, 152–161. doi:10.1002/masy.200950319.

Ugwuja, C. G., Adelowo, O. O., Ogunlaja, A., Omorogie, M. O., Olukanni, O. D., Ikhimiukor, O. O., Iermak, I., Kolawole, G. A., Guenter, C., Taubert, A., Bodede, O., Moodley, R., Inada, N. M., de Camargo, A. S. S. & Unuabonah, E. I. 2019 Visible-light-mediated photodynamic water disinfection @ bimetallic-doped hybrid clay nanocomposites. *ACS Applied Materials & Interfaces* **11**, 25483–25494. Available from: https://pubs.acs.org/doi/full/10.1021/acsami.9b01212 (accessed on 27 June 2023).

Wibuloutai, J., Thongkum, W., Khiewkhern, S., Thunyasirinon, C. & Prathumchai, N. 2023 Microplastics and nanoplastics contamination in raw and treated water. *Water Supply* ws2023116. doi:10.2166/ws.2023.116.

Yang, C., Ye, L., Tian, L., Peng, T., Deng, K. & Zan, L. 2011 Photodegradation activity of polyvinyl chloride (PVC)–perchlorinated iron (II) phthalocyanine (fepccl16) composite film. *Journal of Colloid and Interface Science* **353**, 537–541. doi:10.1016/j.jcis.2010.10.010.

Yang, J., Monnot, M., Sun, Y., Asia, L., Wong-Wah-Chung, P., Doumenq, P. & Moulin, P. 2023 Microplastics in different water samples (seawater, freshwater, and wastewater): Removal efficiency of membrane treatment processes. *Water Research* **232**, 119673. doi:10.1016/j.watres.2023.119673.

Zhang, G. & Musgrave, C. B. 2007 Comparison of DFT methods for molecular orbital eigenvalue calculations. *The Journal of Physical Chemistry A* **111**, 1554–1561. doi:10.1021/jp061633o.

Zhang, K., Hamidian, A. H., Tubić, A., Zhang, Y., Fang, J. K. H., Wu, C. & Lam, P. K. S. 2021 Understanding plastic degradation and microplastic formation in the environment: A review. *Environmental Pollution* **274**, 116554. doi:10.1016/j.envpol.2021.116554.

Zhang, K., Xu, S., Zhang, Y., Lo, Y., Liu, M., Ma, Y., Chau, H.S., Cao, Y., Xu, X., Wu, R., Lin, H., Lao, J., Tao, D., Lau, F. T. K., Chiu, S. C., Wong, G. T. N., Lee, K., Ng, D. C. M., Cheung, S. G., Leung, K. M. Y. & Lam, P. K. S. 2022 A systematic study of microplastic occurrence in urban water networks of a metropolis. *Water Research* **223**, 118992. doi:10.1016/j.watres.2022.118992.

Zhao, Y. & Truhlar, D. G. 2008 The M06 suite of density functionals for main group thermochemistry, thermochemical kinetics, noncovalent interactions, excited states, and transition elements: Two new functionals and systematic testing of four M06-class functionals and 12 other functionals. *Theoretical Chemistry Accounts* **120**, 215–241. doi:10.1007/s00214-007-0310-x.

First received 23 January 2024; accepted in revised form 17 March 2024. Available online 29 March 2024